ChemComm

Accepted Manuscript

This article can be cited before page numbers have been issued, to do this please use: Y. Liu, F. Meng, L. He, X. yu and W. Lin, *Chem. Commun.*, 2016, DOI: 10.1039/C6CC03746A.

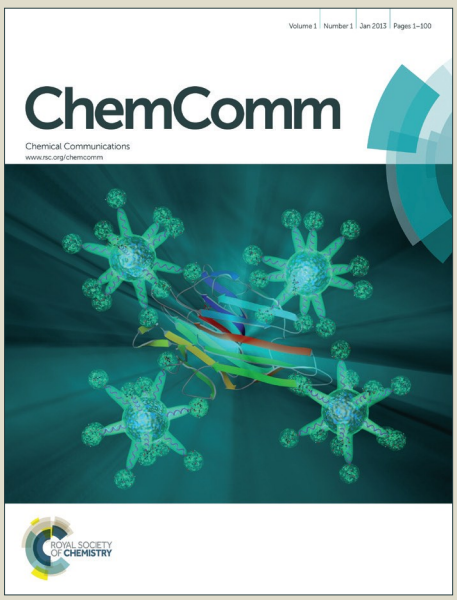

ROYAL SOCIETY OF CHEMISTRY

www.rsc.org/chemcomm

View Article Online
DOI: 10.1039/C6CC03746A

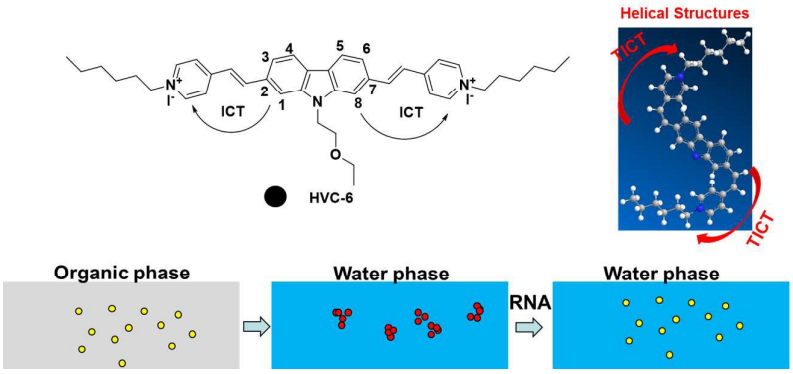

In this work, we developed a unique fluorescent probe **HVC-6** for high sensitive detecting RNA in pure water system and living systems **along with aggregation-disaggregation of probe for the first time**.

View Article Online
DOI: 10.1039/C6CC03746A

Journal Name

COMMUNICATION

Fluorescence behavior of a unique two-photon fluorescent probe in aggregate and solution states and high sensitive detection of RNA in water solution and living systems†

Received 00th January 20xx,
Accepted 00th January 20xx

DOI: 10.1039/x0xx00000x

www.rsc.org/

Yong Liu,[a] Fangfang Meng,[a] Longwei He,[a] Xiaoqiang Yu[b] * and Weiying Lin[a] *

It is found that 2,7-substituted carbazole derivative HVC-6 possesses distinct luminescence feature in both aggregate and solution states. In view of this, the probe HVC-6 realizes high sensitive detecting RNA in pure water system by aggregation-disaggregation method for the first time.

In the past few years, the investigations of conventional small-molecular dyes have made great contributions to the fundamental understanding of luminescence processes at molecular level.[1] The conclusions drawn from the dilute solution data, however, cannot commonly be extended to the concentrated solutions.[2] Thus, aggregation-induced emission (AIE) dyes were discovered by Tang in 2001.[3] Lipophilic AIE molecules form nanoaggregates in aqueous solution spontaneously because of their hydrophobic nature. [3a] These nanoaggregates have been successfully applied for detecting various biological analytes and show more excellent properties than conventional biomaterials.[4] Herein, we describe the development of a unique fluorescent probe for high sensitively monitoring RNA by aggregation-disaggregation method.

Ribonucleic acid (RNA) was made from monomers known as nucleotides.[5] It played central roles in converting genetic information from genes into the amino acid sequences of proteins.[6] RNA was discovered by Friedrich Miescher in 1869,[7] however, the RNA-specific dyes were first used to detect RNA until 1984.[8] More recently, several classes of molecular probes have been developed for RNA detection in living cells.[9] Molecular Probes Co. offers a commercially available RNA probe "SYTO RNA-Select" for RNA imaging in living cells.[10] However, the investigations of RNA probes mainly focus on solution states and lacking investigation of probes. Thus, the goal of our work is to design a unique fluorescent probe for detecting RNA in water with aggregation-disaggregation of probe. We hope this probe possesses higher sensitive to RNA in pure water system and living system than conventional RNA probe (Scheme 1).

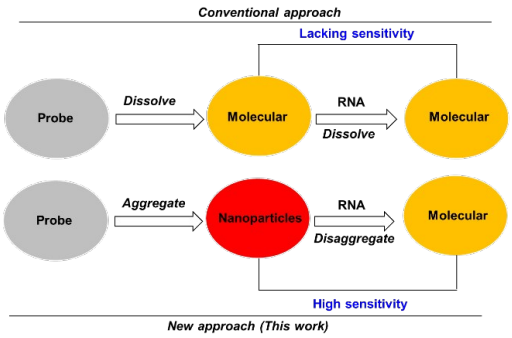

Scheme. 1 Strategies for the sensing of RNA

Toward this end, we herein introduce **HVC-6** (Scheme. 2a) as the first fluorescent dye for high sensitive detecting RNA in pure water by aggregation-disaggregation method. The key to the design is that this novel fluorescent dye should possess distinct luminescence feature in aggregate and solution states. As two-photon (TP) fluorescence is more favorable than one-photon (OP) for imaging applications in living systems,[11] we selected the 2,7-position substituted carbazole derivative as the TP platform. In general, the probe **HVC-6** possessing A-π-D-π-A "Helical Structures'' display aggregate states and weak red fluorescence in aqueous due to twist intramolecular charge transfer (TICT) (Fig. S1†).[12] And similarly structure was capable of detecting nucleic acid based on intercalative binding mechanism.[13] Thus, we envision that the free probe **HVC-6** may exhibit red-shifted emission owing to aggregate of probe. However, in the presence of RNA, the intercalative binding of RNA to **HVC-6** will decrease aggregation of probe and induce a blue-shift in the emission profiles (Scheme 2b).

Chemical synthesis of **HVC-6** is accomplished in a total of five steps (Scheme 2a). The optimization of 4,4'-dibromo-2-nitrobiphenyl (**1**) started from readily available 4,4'-dibromobiphenyl and nitryl. 2,7-Dibromocarbazole (**2**) is steadily

[a] *Institute of Fluorescent Probes for Biological Imaging, School of Chemistry and Chemical Engineering, School of Biological Science and Technology, University of Jinan, Jinan, Shandong 250022, P. R. China. E-mail: weiyinglin2013@163.com*
[b] *Center of Bio & Micro/Nano Functional Materials, State Key Laboratory of Crystal Materials, Shandong University, Jinan, 250100, PR China. E-mail: yuxq@sdu.edu.cn*
Electronic Supplementary Information (ESI) available: Experimental procedures, spectra data, fluorescent imaging and characterization data See DOI: 10.1039/x0xx00000x.

prepared as isolable intermediates for synthesize 2,7-dibromo-9-(2-ethoxyethyl)-9H-carbazole (**3**). HVC is obtained by Heck reaction between **3** and 4-vinylpyridine. Treatment of Iodine hexane with HVC in acetone results in the formation of probe **HVC-6.** The synthetic details of these compounds are shown in the Supporting Information.

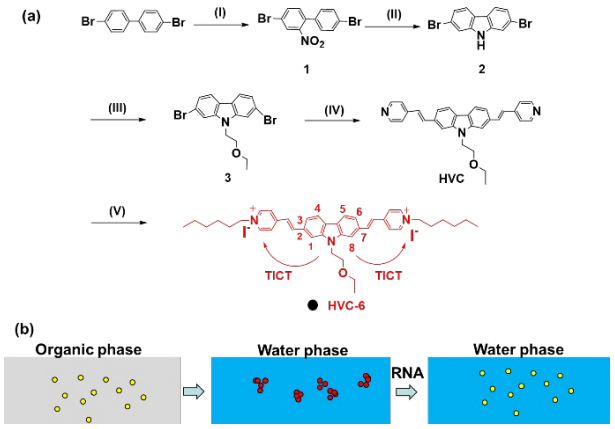

Scheme. 2 (a) Synthesis of probe **HVC-6**; (I) Fuming HNO_3, acetic acid; (II) $P(o\text{-}Et)_3$, Ar; (III) NaOH, DMF, after added 1-bromo-2-ethoxyethane; (IV) Palladium(II) acetate, tri-o-tolylphosphine and K_2CO_3, N-methyl-2-pyrrolidone and 4-vinylpyridine; (V) Acetone, Iodine hexane, reflux; (b) Rational design of the novel TP probe **HVC-6** with distinct fluorescence signals in aggregate and solution states.

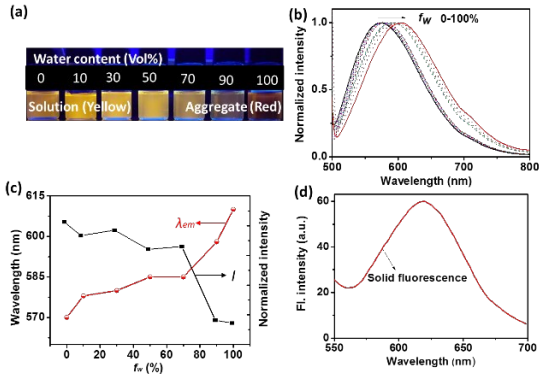

Fig. 1 (a) Photographs of **HVC-6** in water/DMF mixtures were taken under UV illumination; (b) Fluorescence spectra of **HVC-6** in water/DMF mixture; (c) Plots of maximum emission intensity (I) and wavelength (λ_{em}) of **HVC-6** versus water/DMF (f_w, vol %) in water/DMF mixtures; (d) Solid fluorescence spectra of **HVC-6**. Concentration of **HVC-6**: 10 μM. λ_{ex} = 488 nm.

Solid **HVC-6** shows strong red fluorescence at wide-field excitation (Fig. S2†). We envision that the dye **HVC-6** may possess aggregate states in water/DMF mixtures with a high water fraction (f_w). To prove the above assumption, we examine fluorescence behavior of **HVC-6** in water/DMF mixtures . Photographs of **HVC-6** in water/DMF mixtures are taken under UV illumination (Fig. 1a). We systematically change the polarity by admixing polar DMF and water, then we measure the emission spectra of **HVC-6** in solvent mixtures. When f_w increased from 0 (Φ=0.12) to 100% (Φ=0.01), the emission color underwent further hypsochromically shift (Fig. 2b), however, fluorescent intensity is gradually become weak (Fig. 2c). Moreover, solid fluorescence spectrum of **HVC-6** further prove this probe AIE features (Fig. 2d). The above results show that **HVC-6** should be a TICT luminogen with AIE property.[14] Thus, we envision the dye **HVC-6** may form spherical nanoparticles in definite f_w values.

The aggregate characteristics of **HVC-6** are studied by dynamic light scattering (DLS) and transmission electron microscopy (TEM) techniques (Fig. 2). In pure DMF solution, **HVC-6** cannot form aggregate states (Fig. 2a); In water/DMF (f_w = 10%) mixtures solution, the compound **HVC-6** form abundant irregular aggregation (Fig. 2b). Moreover, in water/DMF (f_w = 90%) mixtures solution, the probe **HVC-6** forms spherical nanoparticles with radius 70-100 nm (Fig. 2c). Similar to results of TEM, DLS on 90/10 (f_w = 90%) water/DMF highlight spherical materials with an average size of 70-100 nm (Fig. 2d). The above results further prove that **HVC-6** is luminogen material with AIE property. The results of TEM and DLS techniques are consistent with optical properties of probe in water/DMF mixtures (Fig. 1). We predict this material is capable of detecting intracellular analytes by aggregation-disaggregation method.

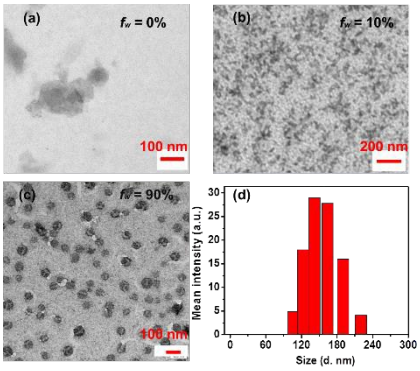

Fig. 2 (a) TEM pictures of water/DMF (f_w = 0%), (b) water/DMF (f_w = 10%) and (c) water/DMF (f_w = 90%) dispersions of **HVC-6** at $2X10^{-5}$ M; (d) DLS measurements of **HVC-6** dispersions in water/DMF (f_w = 90%) mixtures at $2X10^{-5}$ M.

To check the probe **HVC-6** can detect RNA in water solution by aggregation-disaggregation method, fluorescence titration experiments are carried out. First, we set out to investigate the spectral changes of **HVC-6** with increasing RNA. As shown in Fig. 3, when RNA increased to buffer solution of probe, the emission color underwent further hypsochromically shift at 488 nm excitation (Fig. 3a and inset). This phenomenon is similar with photophysical properties of probe in water/DMF mixtures. The fluorescence titration experiments demonstrate that the fluorescence intensity evidently increased at 550 nm with the addition of RNA and show 25-fold enhancement (Fig. 3b). In addition, the probe **HVC-6** present similar results at 800 nm excitation (Figs. 3c and d).

To prove the probe can disaggregation in the presence of RNA in water, DLS experiment is carried out. In water solution (Concentration of **HVC-6** was 10 μM), spherical nanoparticles with the highest value of radius was 250 nm (Fig. S3†); However, in the presence of RNA, radius of spherical nanoparticles decreased to 60

nm. The above results suggest that the probe **HVC-6** can detect RNA in water solution by aggregation-disaggregation method.

To prove sensitivity of probe, we will investigate detection limit of the probe **HVC-6**. Under OP and TP excitation condition, the detection limit for **HVC-6** is calculated to be 0.2 μM (Figs. 4a and b), however, the detection limit of commercially available probe SYTO RNA-Select is 1.8 μM (Fig. S4†), indicating that the probe possesses higher sensitivity than the existing RNA probes.[9]

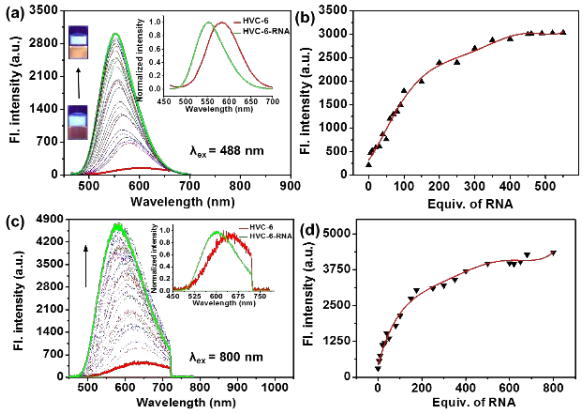

Fig. 3 (a) OP fluorescence spectra of **HVC-6** (10 μM) in tris buffer solution with the addition of RNA (0-550 equiv). Inset: Relative OP fluorescence spectra of **HVC-6** to buffer water solution in the absence and presence of RNA. λ_{ex} = 488 nm; (b) OP fluorescence intensity changes at 570 nm of **HVC-6** (10 μM) with the amount of RNA. λ_{ex} = 488 nm ; (c) TP fluorescence spectra of **HVC-6** (20 μM) in tris buffer solution with the addition of RNA (0-800 equiv). Inset: Relative TP fluorescence spectra of **HVC-6** to buffer water solution in the absence and presence of RNA. λ_{ex} = 800 nm; (d) TP fluorescence intensity changes at 570 nm of **HVC-6** with the amount of RNA. λ_{ex} = 800 nm.

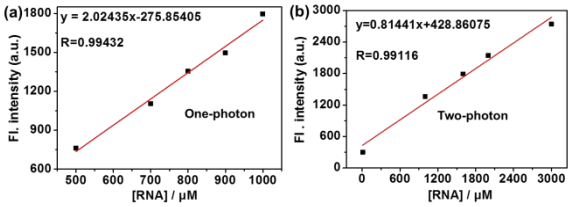

Fig. 4 Normalized response of the (a) OP and (b) TP fluorescence signal by changing the concentration of RNA.

Furthermore, the probe **HVC-6** is treated with various relevant analytes including ions, reactive oxygen species, reducing agents, small molecule thiols, proteins, polysaccharides and nucleic acid in tris buffer solution to investigate the selectivity (Fig. S5†). The addition of the representative anions (Cl^-, HSO_3^-, I^-, NO_2^- and SO_4^{2-}), metal ions (K^+, Mg^{2+}, Ca^{2+} and Zn^{2+}), reactive oxygen and nitrogen species (H_2O_2 and NO_2^-), and reducing agents (SO_3^{2-}) at relevant concentrations induced no marked fluorescence enhancement. Furthermore, the small-molecule thiols such as glutathione (GSH), homocysteine (Hcy), proteins and polysaccharides also elicited no marked response. However, similar with conventional RNA small-molecular probes, the interference of DNA *in vitro* is not ignored.[9]

In order to be useful as imaging agents, fluorescent probes should have low cytotoxicity. Thus, we investigate the potential toxicities of **HVC-6** against HeLa cells. The cytotoxicity of the **HVC-6** probe is evaluated using the standard MTT assays, and the data indicate that the probe has low toxicity for the living cells (Table. S1†). In fluorescent imaging, the red fluorescence of **HVC-6** mainly localizes at the cytoplasm and nucleoli accompanied with faint nuclei distribution rather than cell nucleus. As we all know, the nucleolus contains abundant proteins and RNAs, especially ribosomal proteins and rRNA.[9b] Red fluorescence signals of cells loaded with probe may be caused by endogenous RNA cytoplasm and nucleoli. To verify our assumption, the digest test of ribonuclease (RNase) is carried out. As shown in Fig. S6†, RNase only hydrolyzes the RNA in the cells and did not influence the DNA, is performed. Moreover, the probe **HVC-6** may exist in cells in the form of aggregation after the digest test.

For RNA probes, generally, the interference of DNA *in vitro* is not ignored.[9e] Thus, fluorescence features of the probe should be similar with commercially available probe SYTO RNA-Select *in vitro* and in cells (Fig. 5a). For **HVC-6** and SYTO RNA-Select, *in vitro*, fluorescence response of probe to DNA and RNA in buffer solutions has been investigated (Figs. 5b and c). In living cells, fluorescence of RNA mainly from cytoplasm and nucleoli (Figs. 5d and e). Fluorescence of two probes are stronger than that of DNA. However, *in situ* imaging, the probe **HVC-6** emits stronger fluorescent emission than commercially probe SYTO RNA-Select at the same conditions (Fig. S7†)**.** The above results prove that **HVC-6** can selective imaging RNA in living cells. But, different from SYTO RNA-Select, e **HVC-6** can high sensitively detect RNA by aggregation-disaggregation method.

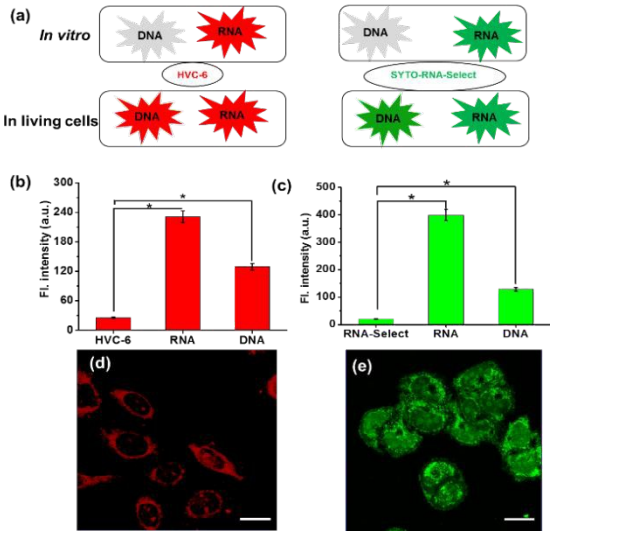

Fig. 5 (a) Fluorescence features of the probe **HVC-6** and commercially available probe SYTO RNA-Select *in vitro* and in living cells; (b) Fluorescence imaging of living cells with **HVC-6** (2 μM); (c) Fluorescence responses (at 550 nm) of **HVC-6** (2 μM) in the presence of RNA and DNA. RNA and DNA concentration: 2.90 mM; (d) Fluorescence imaging of living cells with SYTO RNA-Select (5 μM); (e) Fluorescence responses (at 525 nm) of SYTO RNA-Select (2 μM) in the presence of RNA and DNA, RNA and DNA concentration: 150 mg/mL. λ_{ex} = 488 nm; Scale bar = 20 μm. Statistical analyses were performed with Student's *t*-test (n = 4). * $P < 0.05$.

We further investigate interactions between **HVC-6** and RNA by induced circular dichroism (CD) spectra. As shown in Fig. S8†, CD signal of RNA appear in range of 200-300 nm, and plus and minus two signals confirm spiral chain characteristics of RNA. Due to induction of RNA, cotton peaks of the probe **HVC-6** at 400 (-) and 470 (+) nm corresponded to its absorption peaks bound with RNA. The results demonstrate that **HVC-6** is capable of detecting nucleic acid based on intercalative binding.

Photostability is an important criterion measuring an excellent probe. *In vitro*, the probe exhibits good one- and two-photon photostability (Fig.S9†). Next, we investigate photostability in living cells, commercially available RNA probe SYTO RNA-Select as control. As shown in Fig. 6, SYTO RNA-Select exhibits significant photobleaching with only 40% signal intensity remaining. Fluorescence signals of **HVC-6** only decreased 8%. The results prove that the probe **HVC-6** shows higher photostability than commercially available RNA probe.

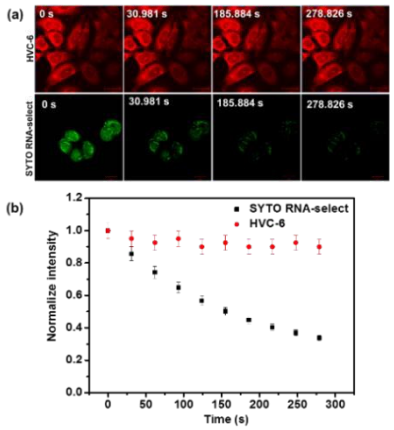

Fig. 6 Comparison of photobleaching of **HVC-6** and SYTO RNA-Select in confocal fluorescence microscopy imaging. Cells stained with 5 μM probe for 30 min; λ_{ex} = 488 nm; λ_{em} = 490-600 nm; Scale bar = 20 μm.

In TP imaging, we have demonstrated that the probe can image RNA in living cells at 800 nm excitation (Fig. S10†). To demonstrate the utility of this probe tissues imaging, the mouse liver tissue slices are treated with the probe **HVC-6**. All of these experiments are performed in compliance with the relevant laws and institutional guidelines, and are approved by the Animal Ethical Experimentation Committee of Shandong University. And fluorescence images of the tissue slices are acquired at 800 nm excitation. Significant fluorescence is observed up to 100 μm in green channel (Fig. S11†). Thus, taken together, the results demonstrate that the probe can image RNA in living tissues.

In summary, we have rationally engineered a novel TP fluorescent probe **HVC-6**, which remarkably display two different emission peaks to aggregate and solution states in the presence and absence of RNA for the first time. And the probe shows sensitivity (Detection limit: 0.2 μM) for monitoring RNA at 488 nm and 800 nm excitation. These unique attributes enable the probe to be employed to one- and two-photon image endogenous RNA in living systems. In addition, compare with commercially available RNA probe SYTO RNA-select, the probe **HVC-6** exhibits higher sensitivity and photostability. We expect that the design strategy might be extended for development of a wide variety of TP functional probes for detecting different RNAs or specific RNA sequence by aggregation-disaggregation method.

Funding was partially provided by NSFC (51503077, 21472067, 21172063), Taishan Scholar Foundation (TS 201511041), doctor start up fund of University of Jinan (160082102). NSFSP (ZR2015PE001), and general start up fund of the University of Jinan.

Notes and references

1 (a) Q. Li, Y. Kim, J. Namm, A. Kulkarni, G. R. Rosania, Y. H. Ahn and Y. T. Chang, *Chem. Biol*., 2006, **13**, 615; (b) J. Yu, D. Parker, R. Pal, R. A. Poole and M. J. Cann, *J. Am. Chem. Soc*., 2006, **128**, 2294.

2 (a) Q. Wan, S. Chen, W. Shi, L. Li and H. Ma, *Angew. Chem. Int. Ed*., 2014, **53**, 10916; (b) M. Yu, X. Wu, B. Lin, J. Han, L. Yang and S. Han, *Anal. Chem*., 2015, **87**, 6688.

3 Y. Hong, J. W. Y. Lam and B. Z. Tang, *Chem. Soc. Rev*., 2011, **40**, 5361.

4 C. W. T. Leung, Y. Hong, S. Chen, E. Zhao, J. W. Y. Lam and B. Z. Tang, *J. Am. Chem. Soc*., 2013, **135**, 62.

5 A. Z. Medvedev, *Adv. Gerontol. Res*., 1964, **21**, 181.

6 E. Robert, Johnston and R. B. Henry, Proc. *Nat. Acad. Sci. USA*., 1972, **69**, 1514.

7 R. Dahm, *Human Genetics*, 2008, **122**, 565.

8 D. A. Melton, P. A. Krieg, M. R. Rebagliati, T. Maniatis, K. Zinn and M. R. Green, *Nuleic. Acids. Res*., 1984, **12**, 7035.

9 (a) S. Cervantes, J. Prudhomme, D. Carter, K. G. Gopi, Q. Li and Y. T. Chang, *BMC. Cell. Biology*., 2009, **10**, 45; (b) Q. Li, Y. Kim, J. Namm, A. Kulkarni, G. R. Rosania, Y.-H. Ahn and Y.-T. Chang, *Chem. Biol*., 2006, **13**, 615; (c) Z. Li, S. Sun, Z. Yang, S. Zhang, H. Zhang, M. Hu, J. Cao, J. Wang, F. Liu, F. Song, J. Fan and X. Peng, *Biomaterials,* 2013, **34**, 6473; (d) S. Zhang, J. Fan, Z. Li, N. Hao, J. Cao, T. Wu, J. Wang and X. Peng, *J. Mater. Chem. B*, 2014, **2**, 2688; (e) G. Song, Y. Sun, Y. Liu, X. Wang, M. Chen, F. Miao, W. Zhang, X. Yu and J. Jin, *Biomaterials*, 2014, **35**, 2103; (f) L. Li, J. Feng, H. Liu, Q. Li, L. Tong and B. Tang, *Chem. Sci.*, 2016, **7**, 1940.

10 R. P. Haugland, in *the handbook, A Guide to Fluorescent Probes and Labeling Technologies*, ed. M. T. Z. Spence, 10tH., 2005, pp.710-711.

11 (a) H. Yu, Y. Xiao and L. Jin, *J. Am. Chem. Soc*., 2012, **134**, 17486; (b) H. -Y. Ahn, K. E. Fairfull-Smith, B. J. Morrow, V. Lussini, B. Kim, M. V. Bondar, S. E. Bottle and K. D. Belfield, *J. Am. Chem. Soc*., 2012, **134**, 4721; (c) Y. H. Lee, W. X. Ren, J. Han, K. Sunwoo, J. -Y. Lim, J. -H. Kim and J. S. Kim, *Chem. Commun.*, 2015, **51**, 14401.

12 Y. Zhang, J. Wang, P. Jia, X. Yu, H. Liu, X. Liu, N. Zhao and B. Huang, *Org. Biomol. Chem.*, 2010, **8**, 4582.

13 T. Y Ohulchanskyy, H. E. Pudavar, S. M. Yarmoluk, V. M. Yashchuk, E. J. Bergey, P. N. Prasad, *Photochem. Photobiol.*, 2003, **77**, 138.

14 X. Y. Shen, W. Z. Yuan, Y. Liu, Q. Zhao, P. Lu, Y. Ma, I. D. Williams, A. Qin, J. Z. Sun and B. Z. Tang, *J. Phys. Chem. C.*, 2012, **116**, 10541.